

Supplementary Material

Probing mechanical properties of graphene oxide/epoxy composites based on nano indentation technique

Cun Zhao^a, Yufen Zhao^b, Xiaoyuan Pei^a, Shengkai Liu^{a,*}, Yuanhua Xia^c, Chunying Min^d, Ruiqi

Shao^a, Chunhong Wang^a, Wei Wang^a, Zhiwei Xu^{a,*}

^a Key Laboratory of Advanced Braided Composites, Ministry of Education, School of Textile

Science and Engineering, Tiangong University, Tianjin 300387, China

^b AECC Aegis Advanced Protective Technology Co., Ltd, Tianjin 300300, China

^c Key Laboratory of Neutron Physics, Institute of Nuclear Physics and Chemistry, China

Academy of Engineering Physics, Mianyang 621999, China

^d Research School of Polymeric Materials, School of Materials Science & Engineering, Jiangsu

University, Zhenjiang, Jiangsu, 212013, China

1. Nanoindentation testing details

Nanoindentation, also known as depth sensitive indentation, was first proposed as a measurement tool by Oliver et al. in 1992. In 2004, when calculating hardness by Oliver & Pharr method, the hardness (H) can be defined by the following formula (Eq. (1) (2)).

$$H = P_{max}/A_c \quad (1)$$

$$A_c = 24.56 \times h_c^2 \quad (2)$$

* Corresponding author, e-mail addresses: liushengkai@tiangong.edu.cn (S. Liu), xuzhiwei@tiangong.edu.cn (Z. Xu).

Here, P_{max} is the maximum indentation load (N), A_C is the indentation contact area (mm^2), H is the indentation hardness of the material (GPa), and h_C is the load displacement (nm). The effect of adding KH-GO nanoparticles on nanomechanical properties such as hardness of the samples was studied using Nano-indenter (TI980 TriboIndenter, Bruker) by utilizing a Berkovich type indenter. Nanoindentation tests were performed under load control with maximum load of 1000 μ N. The test started as sample surface approached to indenter. Once the surface contact was detected, the indenter was pressed into sample at strain rate of 200 μ N/s until the defined load of 1000 μ N was achieved. At maximum load, the load was held for 2 s, followed by an unloading process at the same rate until load was removed completely. All the data were analyzed using built-in software.

2. Dispersion stability of KH-GO in acetone

As for the dispersion of functionalized GO in acetone, supplementary instructions were made as follows: Appropriate amount of functionalized GO was weighed and dissolved in acetone, and a solution with a concentration of 0.5 mg/ mL was prepared. Ultrasonic treatment was first performed on the mixed solution (parameters: Ultrasonic power, 2800 W, Ultrasonic time, 1h). Then the solution was further peeled and dispersed by a high-pressure homogenizer (NanoGenizer30K, Genizer LLC, USA: The pressure 2.4 kpsi, and the number of cycles 3), and the mixture was uniformly dispersed. The mixed solution was left standing and the sinking situation of functionalized GO in acetone was photographed and observed and compared at 3, 6, 12, 24 and 36 h.

The figure shows the dispersion of KH-GO in acetone at different time periods. Appropriate amount of KH-GO was added to acetone for ultrasonic dispersion for 1 h and then stood for 36 h to observe its dispersion effect. KH-GO stood for 3 h in solvent acetone, and remained in a good dispersion state for 6 h, with a small amount of precipitation at 12 h and more precipitate at 24 h. The subsidence of 36 h is basically the same as that of 24 h. In summary, it indicates that KH-GO has good

compatibility with acetone, and after curing with thermosetting resin, KH-GO will show good interface properties.

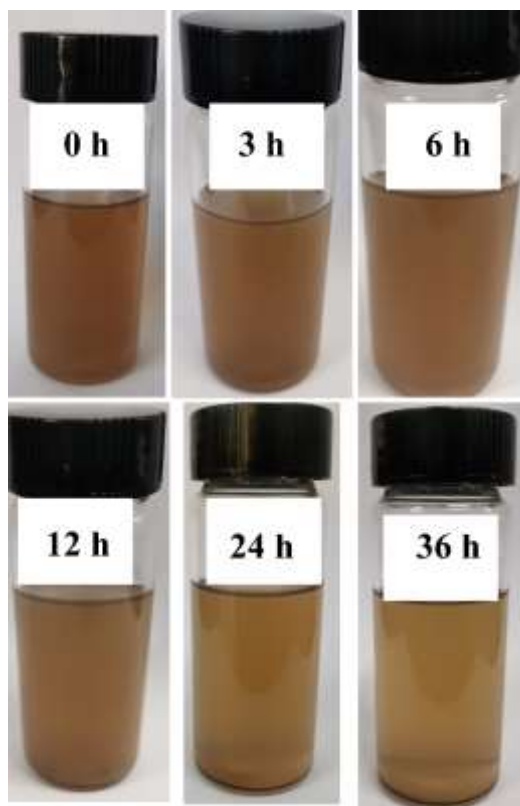


Fig. S1. Dispersion of KH-GO in acetone

3. Microstructural characterization of composite materials

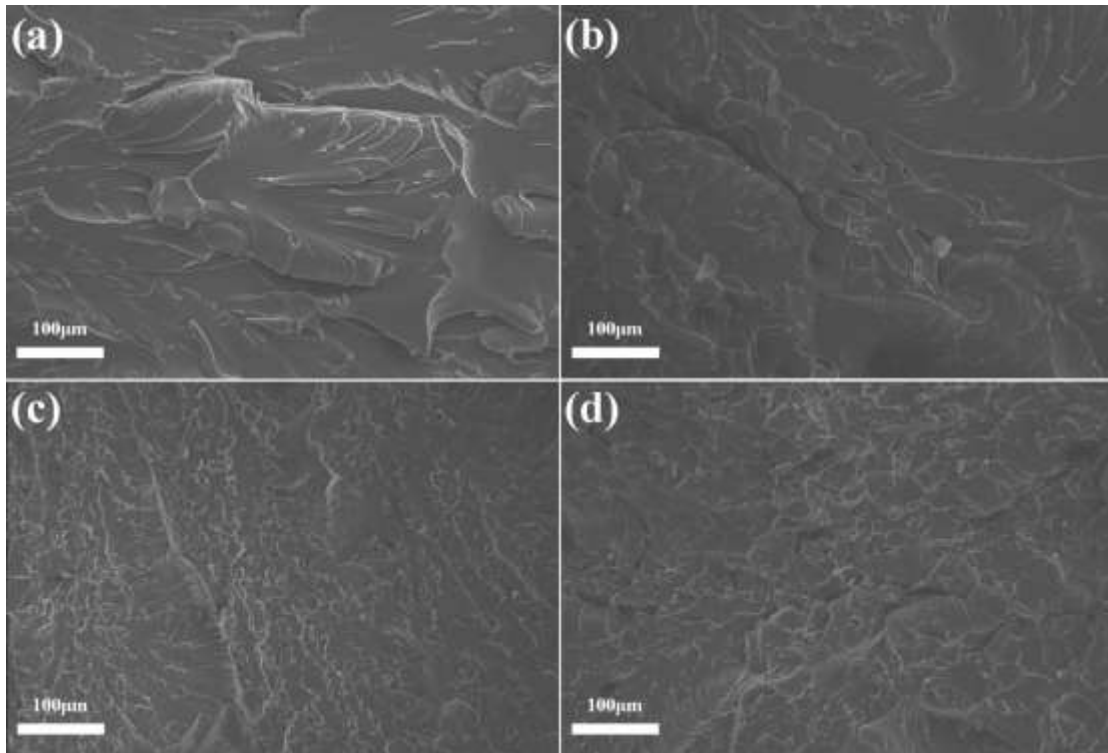


Fig. S2. Cross-sectional SEM images of freshly fractured surfaces of KH-GO/EP composites. (a) neat EP, (b) 0.1wt%, (c) 0.3wt%, (d) 0.5wt%.

As can be seen from Fig. S2, the fracture surface of pure resin was relatively smooth and flat, with a small number of ripples. The ripples could be seen to be sharp and angular, reflecting the characteristics of brittle fracture. The results are consistent with those observed by SEM at 20-micron scale. With the increase of the addition of KH-GO, it is obvious that the fracture surface of composite material gradually changed from the brittle fracture of sharp to the fracture surface of small massive fish scales. These cracks and fragments amplify the elastic energy dissipation in crack propagation by causing damage distribution in a greater area in the resin. This is attributed to GO's effective role in deflecting crack paths and increasing toughening mechanisms at the microscale. When the dosage of KH-GO was 0.3wt%, the formed scale-like cracks were the densest.

4. The morphological tests of nanoparticles

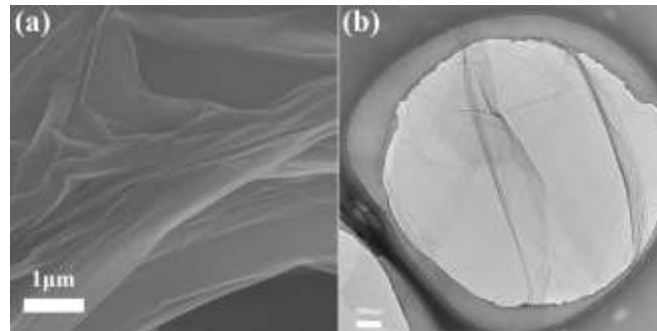


Fig. S3. SEM (a) and TEM (b) images of HK-GO.

Fig. S3 shows the representative SEM and TEM images of KH-GO. It can be clearly seen from SEM and TEM images that the KH-GO slices show some thin ripples on the clean surface. These folds are beneficial to improve the interfacial adhesion between nanoparticles and polymer matrix, improve the dispersion of nanoparticles, and further improve the properties of composites.

5. The characterization of nanoparticles (Raman, TGA, AFM)

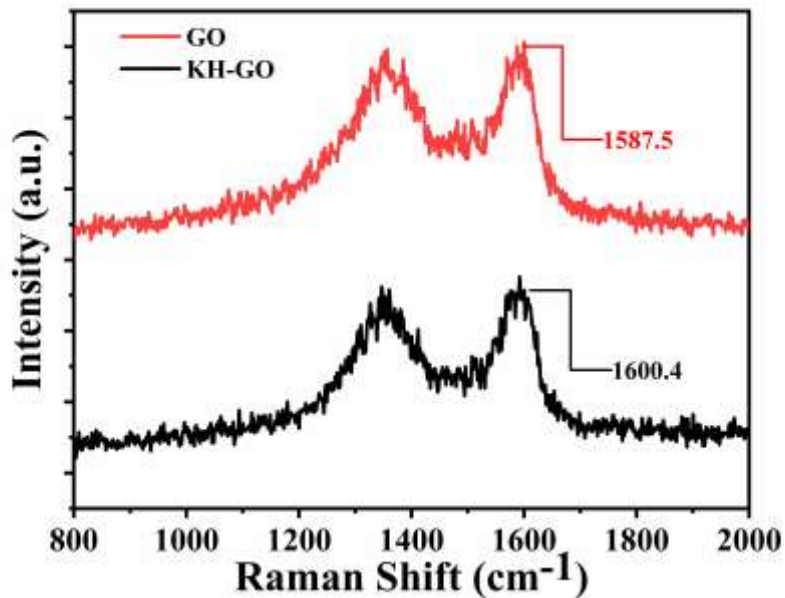


Fig. S4 the Raman spectra of graphite oxide and KH-GO

Fig. S4 presents the Raman spectra of graphite oxide and KH-GO. As shown in the figure, the G band is broadened and shifted to 1587.5 cm⁻¹ for the graphite oxide, and markedly shifted to 1600.4 cm⁻¹ after silane functionalization, implying a better exfoliation of graphene layers.

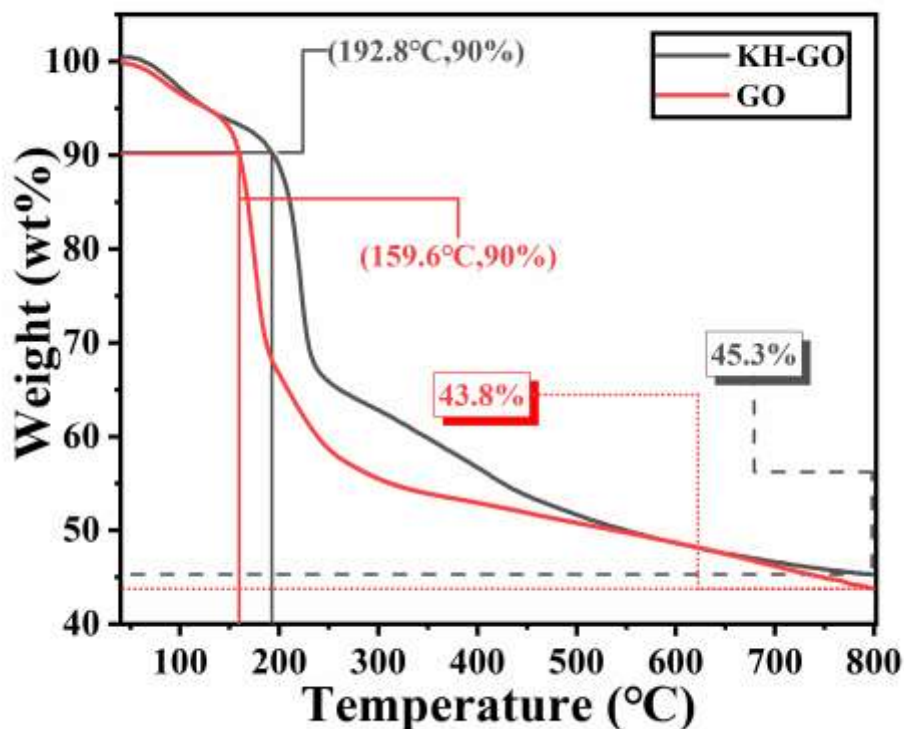


Fig. S5 Thermal weightlessness of GO and KH-GO

Fig. S5 presents the TGA curves of graphite oxide and KH-GO. When the sample weight loss is 10%, it can be found that the temperature of GO corresponds to 159.6 °C, while that of KH-GO increases to 192.8 °C. which is likely due to the pyrolysis of the unstable oxygen functionalities (such as the hydroxyl, Carbonyl, and carboxylic groups), generating gases including CO, CO₂, and steam. When the temperature reaches 800 °C, the residual mass of GO is 43.8%, and the residual mass of KH-GO is 45.3%. By comparison, the KH-GO exhibits better thermal stability.

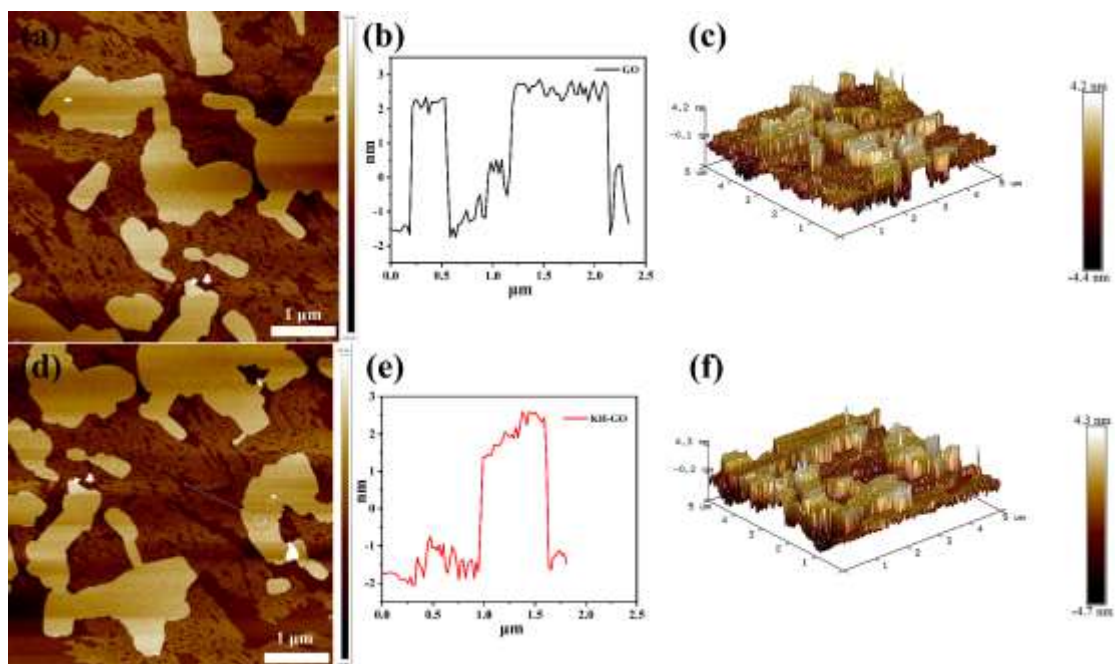


Fig. S6 AFM images, thickness and three-dimensional height profiles of (a) (b) (c) GO and (d) (e) (f) KH-GO.

Table S1 Average surface roughness and root mean square roughness of each sample.

Name	GO (nm)	KH-GO (nm)
Rq	1.39	1.54
Ra	1.11	1.24

To observe the morphology and measure the thickness of the GO and KH-GO, AFM measurements were conducted. The images of GO and KH-GO are shown in Fig. S6 (a) (b) (c) and (d) (e) (f), respectively. The average thickness of the GO sheets is 4 nm. In the case of KH-GO, the average thickness is 5 nm. Suggesting the presence of silane-functionalized groups on the GO sheets. The root mean square roughness of GO is 1.39 nm, while the root mean square roughness of KH-GO is 1.54 nm, indicating that the roughness of functionalized GO increases.